

Investigation of depth dependent changes in cerebral haemodynamics during face perception in infants

A Blasi¹, S Fox², N Everdell¹, A Volein², L Tucker², G Csibra², A P Gibson¹, J C Hebden¹, M H Johnson² and C E Elwell¹

¹ Biomedical Optics Research Lab, Department of Medical Physics and Bioengineering, Malet Place Engineering Building, University College London, London WC1E 6BT, UK

² Centre for Brain and Cognitive Development, Henry Wellcome Building, Birkbeck College, University of London, Malet Street, London WC1E 7HX, UK

E-mail: ablasi@medphys.ucl.ac.uk

Abstract. Near infrared spectroscopy has been used to record oxygenation changes in the visual cortex of 4-month-old infants. Our in house topography system, with 30 channels and 3 different source-detector separations, recorded changes in the concentration of oxy-, deoxy- and total haemoglobin (HbO₂, HHb and HbT) in response to visual stimuli (face, scrambled visual noise and cartoons as rest). The aim of this work was to demonstrate the capability of the system to spatially localise functional activation and study the possibility of depth discrimination in the haemodynamic response. The group data show both face stimulation and visual noise stimulation induced significant increases in HbO₂ from rest, but the increase in HbO₂ with face stimulation was not significantly different from that seen with visual noise stimulation. The face stimuli induced increases in HbO₂ were spread across a greater area across all depths than visual noise induced changes. In results from a single subject there was a significant increase of HbO₂ in the inferior area of the visual cortex in response to both types of stimuli, and a larger number of channels (source-detector pairs) showed HbO₂ increase to face stimuli, especially at the greatest depth. Activation maps were obtained using 3D reconstruction methods on multi source-detector separation optical topography data.

Keywords: NIRS, optical topography, infant functional brain development, visual cortex.

1. Introduction

Near infrared spectroscopy has been used extensively to monitor changes in the concentration of oxy and deoxyhaemoglobin resulting from neural activity in the human brain (Obrig and Villringer 2003, Hoshi 2003, Koizumi *et al* 2003, Aslin and Mehler 2005, Bunce *et al* 2006). The technique is non-invasive, affordable, and portable. It has found widespread application in studying brain function in infants during visual (Meek *et al* 1998), auditory (Sakatani *et al* 1999,

Nissila et al 2004), olfactory (Bartocci et al 2000) and motor (Hintz et al 2001) stimulation. More recently NIRS has been used to investigate the neural basis of more complex cognitive abilities during the first year of life (Baird et al 2002, Wilcox et al 2005, Csibra et al 2004, Peña et al 2003, Minagawa-Kawai et al 2007, Bortfeld et al 2007), with a view to characterising functional brain development.

Current state of the art of NIRS technology is limited to measurement of the haemodynamic activation of the outer layer of the cortex, as shown by Monte Carlo simulation of near infrared light propagation on models of the adult head (Okada et al 1997). However, whereas in adults the spatial profile of near infrared light remains quite superficial, i.e., in the grey matter of the cortex., in the neonate head, an increase in source-detector spacing increases the interrogated volume of tissue into deeper layers (Fukui et al 2003). This provides an opportunity to extend the use of NIRS technology into the field of developmental cognitive neuroscience (where techniques such as positron emission tomography (PET) and functional magnetic resonance imaging (fMRI) have more limited application). For these studies it is necessary to interrogate regions beyond the superficial layers of the cortex and to introduce depth discrimination into NIRS functional activation measurements.

There have been several studies that have used near infrared spectroscopy to investigate haemodynamic responses to visual stimuli in the occipital cortex of human infants. To date the majority of these studies have used simple stimuli such as a chequerboard or white light (Kusaka et al 2004, Hoshi et al 2000, Taga et al 2003). There is however a substantial body of evidence measuring neural correlates of face perception in infants using behavioural and ERP methods (Halit et al 2003, de Haan et al 2002, Tzourio-Mazoyer et al 2002). Faces are so important to humans that we have specialised brain areas for processing them (Kanwisher et al 1997). Newborn infants orient to schematic face stimuli (Farroni et al 2005) and can discriminate faces

within the first days of life (Pascalis *et al* 1995). In a previous study we used stimuli of face and scrambled face photographs to investigate responses in the occipital cortex (Csibra *et al* 2004). This study demonstrated that NIRS could be used to detect haemodynamic activation in response to faces in both infants and adults. However spatial localisation of the activation was fairly limited, as only a 2 channel system was used, with probes positioned one pair on the frontal and the other pair on the visual cortex (NIRO 300, Hamamatsu Photonics).

Over the last decade a number of optical topography systems have been developed that allow multiple measurements of attenuation over a large area of tissue (Yamashita *et al* 1999, Takahashi *et al* 2000, Franceschini *et al* 2003, Everdell *et al* 2005, Kusaka *et al* 2004, Colier *et al* 2001). However, the two dimensional maps produced by most optical topography systems originate from equally spaced source-detector pairs and provide no depth information. NIR tomography data can be used for 3D image reconstruction (Benaron *et al* 2000, Bluestone *et al* 2001, Gibson *et al* 2006), which can in turn be integrated with functional magnetic resonance imaging (Zhang *et al* 2005) for better localisation of the activation. Although optical tomography has the capability to provide full 3D images, the acquisition time of the system is typically in the region of minutes and the heavy attenuation of light across the infant head restricts its use to measurements in neonates (with less than 11cm head mean diameter).

Our NIR optical topography system has a sensor pad array of 16 laser diode sources (8 at 780 nm and 8 at 850 nm) and 8 avalanche photodiode detectors (Everdell *et al* 2005) and uses a frequency multiplexed approach to record signals from all sources that a detector can receive light from. We can therefore record from up to 30 source-detector pairs (or channels) with only 8 source and 8 detector points. We have designed the distribution of the source and detector points on the sensor pad not only to maximise the number of channels, but also to include three different source-detector separations interrogating three different depths within the infant head.

The aim of this study was to investigate haemodynamic responses to a complex visual stimulus in 4-month-old babies by using our in-house topography system with 30 channels and 3 different source-detector separations to cover not only a large portion of the surface of the visual cortex but also to interrogate different depths within the cortex.

2. Methods

2.1. Subjects

Data were recorded from 12 healthy 4-month-old babies (6 boys and 6 girls, mean \pm SD age 126 \pm 6 days) at the Centre for Brain and Cognitive Development Babylab, Birkbeck, University of London. A total of 38 babies were selected to participate in the study, although 26 babies had to be excluded from the analysis because of excessive head movement and/or failure to look at the stimulus for a sufficient length of time. Ethical approval was obtained for this study from the local ethics committee and informed written consent was obtained from all the parents.

2.2. Protocol

The protocol used in our studies was similar to that used in a previous study in which measurements were made with 2 source-detector pairs (Csibra *et al* 2004). The babies sat comfortably on their parent's lap facing a video screen and were encouraged to watch the screen for as long as possible. The stimuli were presented in a cyclic loop, starting with animated cartoons to attract the babies' attention. After at least 10 seconds of cartoons, 10 different face images were presented at a rate of one per second. This was followed by at least 10 seconds of cartoons, after which 10 visual noise images were presented, again at a rate of 1 per second. For each trial, the infants had to look continuously for a minimum of 4 seconds to the cartoons before either the face or noise stimuli were presented.

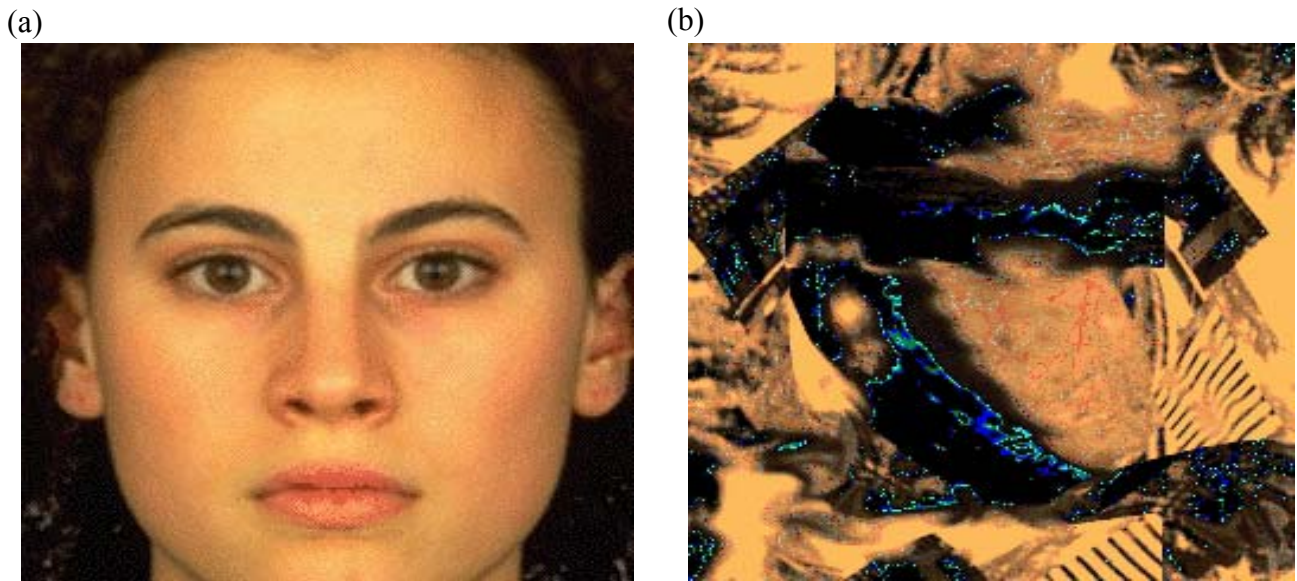


Figure 1: Example of (a) FACE and (b) NOISE stimuli used in the study

Face stimuli were full colour images of five female faces and visual noise stimuli were artificially constructed images with the same spatial frequencies and colour distribution as the faces (Goffaux *et al* 2003, see figure 1). The study lasted for as long as the baby was willing to look at the images (typically between 3 and 12 minutes).

2.3. Instrumentation

NIRS data were recorded using the UCL topography system (Everdell *et al* 2005), with a sensor pad of 16 sources (8 at 780 nm and 8 at 850 nm), which are illuminated simultaneously and 8 detectors operating in parallel. The system uses a frequency multiplexed approach allowing rapid data acquisition with good signal to noise ratio (56 dB) and flexibility in the source detector geometry used in the array. Fourier transform software is employed to demultiplex multiple source signals which are each modulated at a different frequency ranging from 2 kHz to 4 kHz. The frequencies are kept within one octave to avoid interference from harmonics. The mean power emitted by each laser diode was approximately 2 mW. Each source and detector was coupled to the scalp via a 1 mm diameter multimode optical fibre. For these studies, a custom made optode array was designed as shown in figure 2.

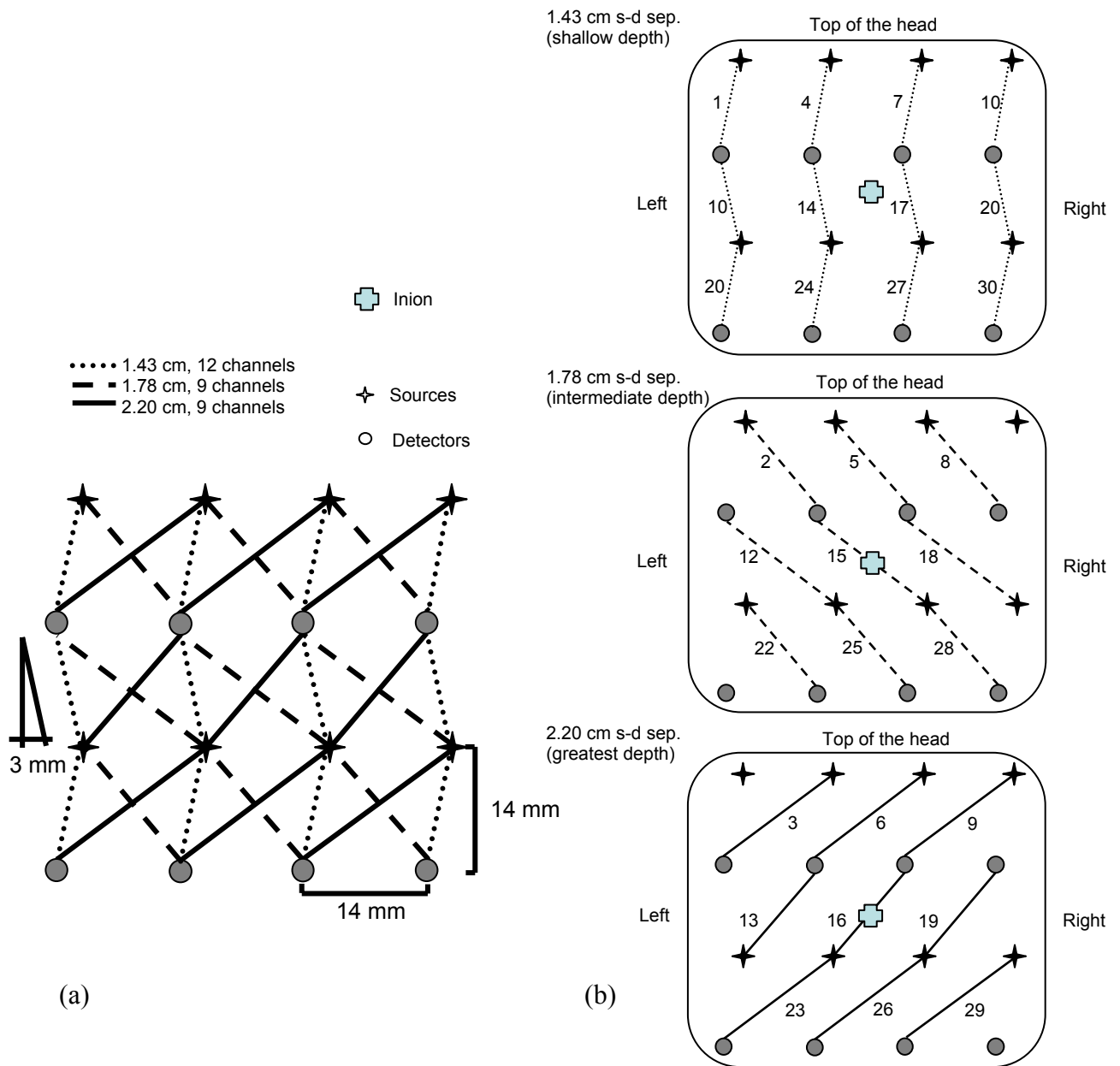


Figure 2: (a) Optode array design incorporating three source-detector separations. (b) Source-detector pairs at each spacing, and their position on the back of the subject's head with Oz (international 10/20 system, represented with a blue cross) as a reference. Note that the intermediate and large source-detector separation channels share the same midpoint, but the region probed does not coincide. Also, the channels with shorter source-detector separations are placed in slightly different regions to the intermediate and largest source-detector channels.

The 8 source optodes and 8 detector optodes were arranged to allow recording from a total of 30 channels (source-detector pairs) with 12 channels having a source detector spacing of 1.43 cm, 9 channels having a source detector spacing of 1.78 cm and 9 channels having a source detector spacing of 2.20 cm. The 12 channels with source-detector separations of 1.43 cm were assumed to be interrogating nearest to the surface depth (referred as shallow depth), the 9 channels with source-detector separations of 1.78 cm were assumed to be interrogating mid depth (intermediate depth), and the 9 channels with source-detector separations of 2.20 cm were assumed to be interrogating furthest from the surface depth (greatest depth).

The optodes were held in the array using a lightweight aluminium shell lined with soft light absorbing foam, which was held on the head using a Coban strap (figure 3). The centre of the array was positioned over the visual cortex between O1 and O2 (10-20 electrode placement system, Jasper 1958). NIRS data were acquired at 10Hz.

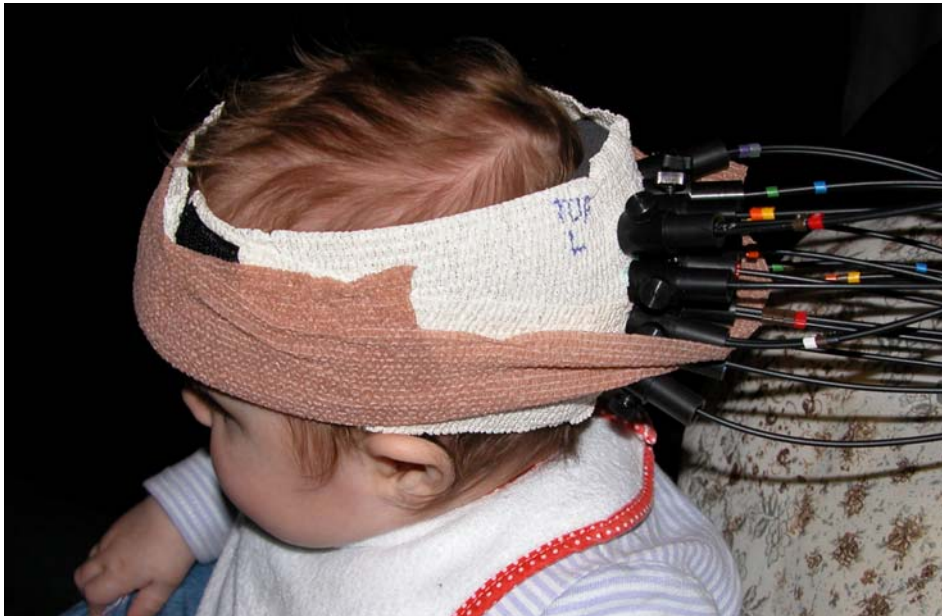


Figure 3: Photograph of optode array fixed over the occipital cortex of a four month old infant.

2.4. Behavioural monitoring

A video recording was made of each infant. Following the study, the video was reviewed by an experimenter who coded the amount of time the babies looked at each stimulus. This was the first step in the selection of valid trials. For a trial to be considered valid, the baby had to be looking at the screen for at least 4 seconds prior to the stimulus onset and then look for at least 8 seconds during the presentation of the stimulus. Trials during which the infant was not attending to the screen or where there was excessive head movement were rejected from further analysis. A minimum of four trials with each type of stimulus were required to include a baby in the study.

2.5. Data Processing

2.5.1. Data rejection: The recorded attenuation measurements for each data set were initially inspected and channels that showed evidence of poor signal to noise ratio ($\text{SNR} < 5 \text{ dB}$, measured in the 4 sec pre-stimulus onset period) together with a large standard deviation in the rest period across all trials ($> 1.8 \mu\text{M}$), mismatch in attenuation at the two wavelengths (possibly due to the foam from the pad obstructing one of the fibres in the source optode, evaluated by comparing the variability of the attenuation signal from each wavelength in the rest period) or saturation of the detector (detection of physiologically unrelated oscillations around 1 Hz by spectral analysis), were rejected from further analysis. The average number of channels rejected per baby was 6, with a minimum of 1 channel rejected (in 1 baby) and a maximum of 9 channels rejected (in 2 babies). If the rejected channels were all clustered around a specific area of the pad for the same source-detector separation, the baby was excluded from the study. At most, 3 neighbouring channels were allowed to be rejected for each depth, with a total maximum of 10 channels for a single baby.

2.5.2. Data analysis: For each participant, the signal was low-pass filtered and divided into 24 s sections. Each section consisted of 4 s of rest prior to stimulus presentation, (pre-stimulus baseline); 10s of stimulus (either face or noise) and 10 s of rest post-stimulus (post stimulus

baseline). For each of these sections, the attenuation data was detrended with a linear fit between the first and last 4 seconds of the block, where we assumed all stimulus effects on the signal had subsided. Then, the pre-processed data was converted into changes in the concentration of HbO₂ and HHb using the modified Beer Lambert law and assuming a differential pathlength factor for infants (Duncan et al 1995). For each infant we averaged trials grouped by stimulus type and we obtained a time course of the mean change in HbO₂ and HHb at each channel and for each stimulus type. Statistical comparisons were made within each channel between baseline (zero) and maximum increase of HbO₂, HHb and HbT (= HbO₂ + HHb) with each stimulus type for the group of infants with good data for that particular channel. Further analysis of the channels with a significant increase of the signals was conducted to compare the maximum increase of HbO₂ between the 2 types of stimulus. One baby was selected as representative of the responses to the presented stimuli. Maximum HbO₂ increase was analysed for this subject and a 3D reconstruction of the activation was carried out. It must be noted that it was necessary to present cartoons in the rest period in order to keep the infants' attention on the screen. The significant signal changes quoted in the results are therefore changes from this "rest" condition in which cartoons were presented.

2.5.3. *Image reconstruction:* The multiple source-detector separations available from this array allow for three-dimensional (3D) tomographic image reconstruction which provides better overall image quality than the more usual two-dimensional mapping technique (Boas *et al* 2004). We chose to reconstruct 3D images using the Rytov approximation (Arridge 1999) in which measured changes in log(amplitude), Δy , are assumed to be related to changes in the optical absorption, Δx , by the matrix equation $\Delta y = A\Delta x$, where A is the Jacobian or sensitivity matrix. A was calculated using a software package known as TOAST (Arridge *et al* 2000) by solving the diffusion equation using the finite element method applied to a finite element mesh of tetrahedra with quadratic interpolation functions, which was generated using Netgen (Schöberl 1997). Images were generated by Tikhonov regularisation of the Moore-Penrose generalized inverse $\Delta x = A^T(AA^T + \lambda$

$I)^{-1}\Delta y$, where the regularization parameter λ was set to 10% of the largest singular value of AA^T and I is the identity matrix.

3. Results

For each source-detector pair, we obtained one time series of the change in HbO_2 , HHb and HbT per baby. We measured the maximum increase of each with respect to the pre-stimulus baseline level in the interval between 4 and 13 sec post-stimulus onset. Analysis of HbO_2 increase (group averaged) showed that in face trials, (a) at the shallow depth, there was a significant increase in the signal in 3 channels, most clustered in the inferior part of the pad; (b) there was only one channel at the intermediate depth with a significant HbO_2 increase; and (c) at the largest source-detector separation, 4 channels showed a significant signal increase. Additionally, at the greatest depth, 2 channels also had an increase in HbT . Figure 4 shows the channels with HbO_2 and joint $HbT-HbO_2$ significant increases with face and noise stimulation. Although not reflected in figure 4, 2 channels at the greatest depth (13 and 23) also showed an increase in HHb . The same analysis performed in noise trials found a significant increase in HbO_2 in 1 channel, the same one at intermediate depth where an HbO_2 increase was detected with face stimulation. HbT increased in channels 17 (shallow depth) and 6 (greatest depth), whereas HHb increased in channels 2 (intermediate source-detector separation) and 6. It is interesting to note that where there was an increase in HbO_2 , HbT did not necessarily change. Our results show that HbO_2 is the chromophore with most sensitivity to change after stimulation, therefore our results from now on will focus on changes in HbO_2 . Time of peak range of HbO_2 in face trials at the channels where its increase was significant was between 5.1 and 11.6 sec after stimulus onset. The corresponding range for noise trials was between 7.3 and 11.5 sec.

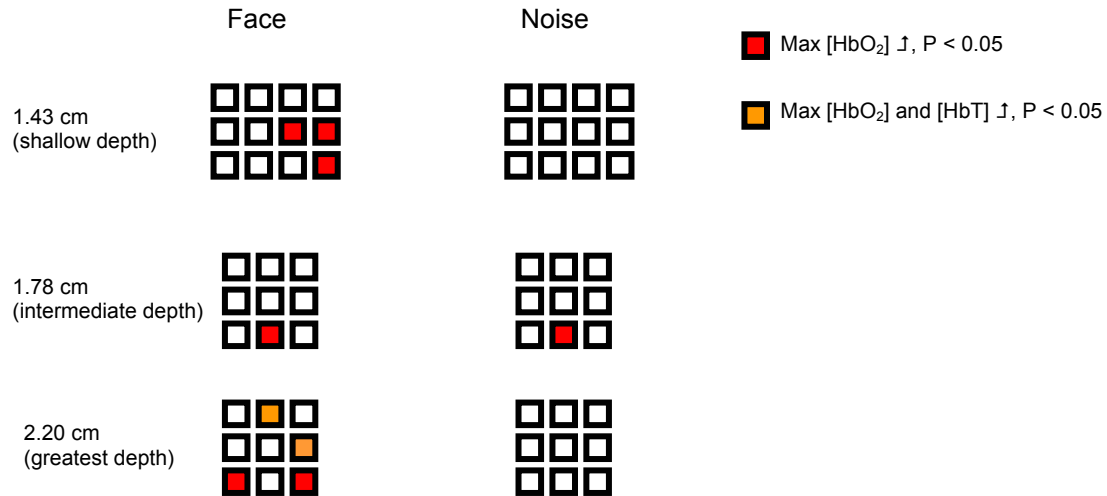
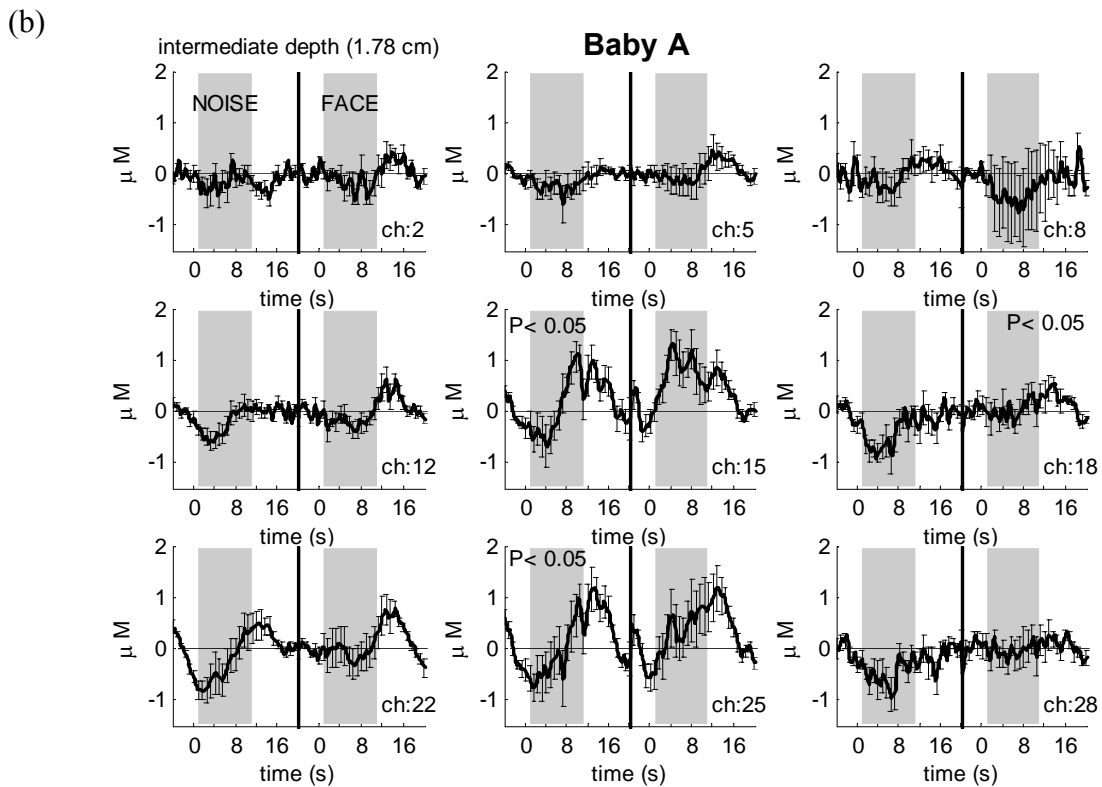
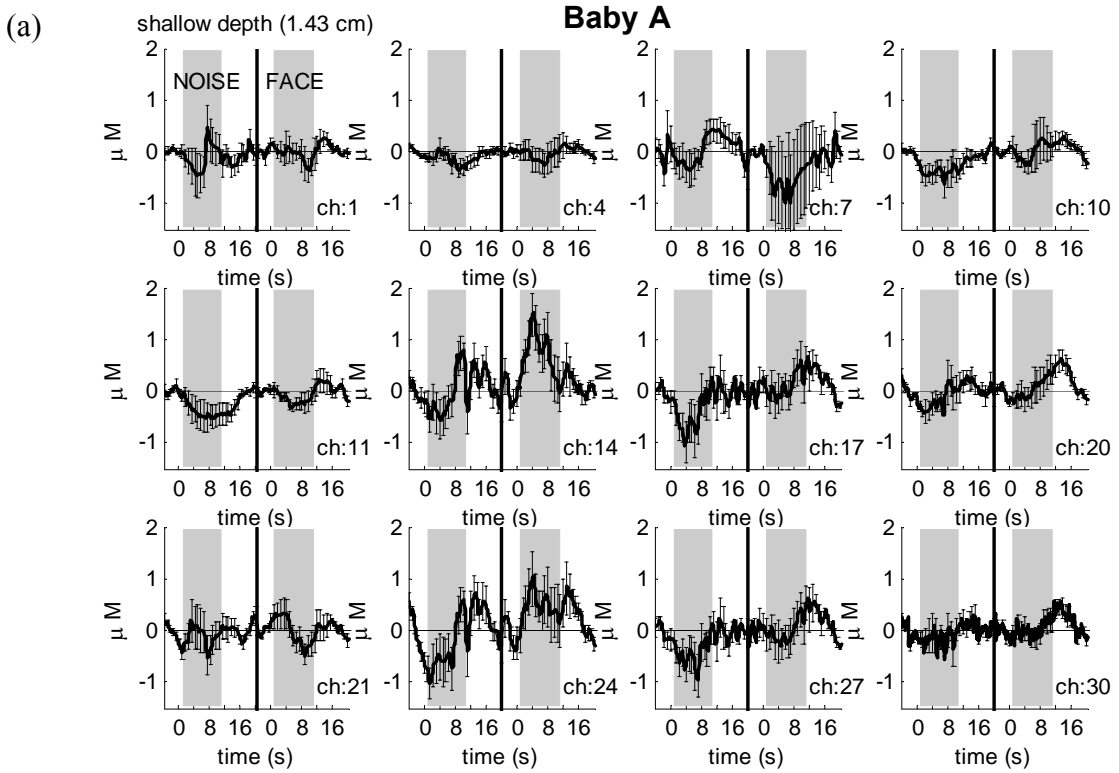


Figure 4: Map of channels for group data, at each source-detector separation, showing significant maximum increase in HbO_2 and joint HbO_2 - HbT for FACE and NOISE stimuli. For each channel, we obtained a set of maximum signal increase values, one per infant. Then, within each channel, we tested whether the maximum increase was significantly different from zero.

Post-hoc analyses of the maximum increase in HbO_2 in face and noise trials on the channels shown in figure 4 with paired T-test only detected a significantly different increase in face vs. noise trials ($P < 0.05$) in channel 6, at the greatest depth. Analysis of the time course of HbO_2 between 4 and 13 sec post-stimulus onset with 2-way repeated measures analysis of the variance using “time” and “trial” as factors, shows a significant effect of “time X trial” in channels 17 (shallow depth, $P < 0.001$), 25 (intermediate depth, $P = 0.020$) and 23 (greatest depth, $P < 0.001$), suggesting the change in time of the signal depends on the type of stimulus.

Statistical comparison of haemodynamic activation across infants may conceal important effects in the results because (a) there may be differences in the location of peak activation between babies, (b) the signal change may have had a different time course in different babies, and because of (c) the slight variations in the exact position of the probe on the infants head. For this

reason we present an analysis for a single infant (identified as baby A), who was chosen because there were sufficient number of face (8) and noise (9) trials for statistical power in her recording.



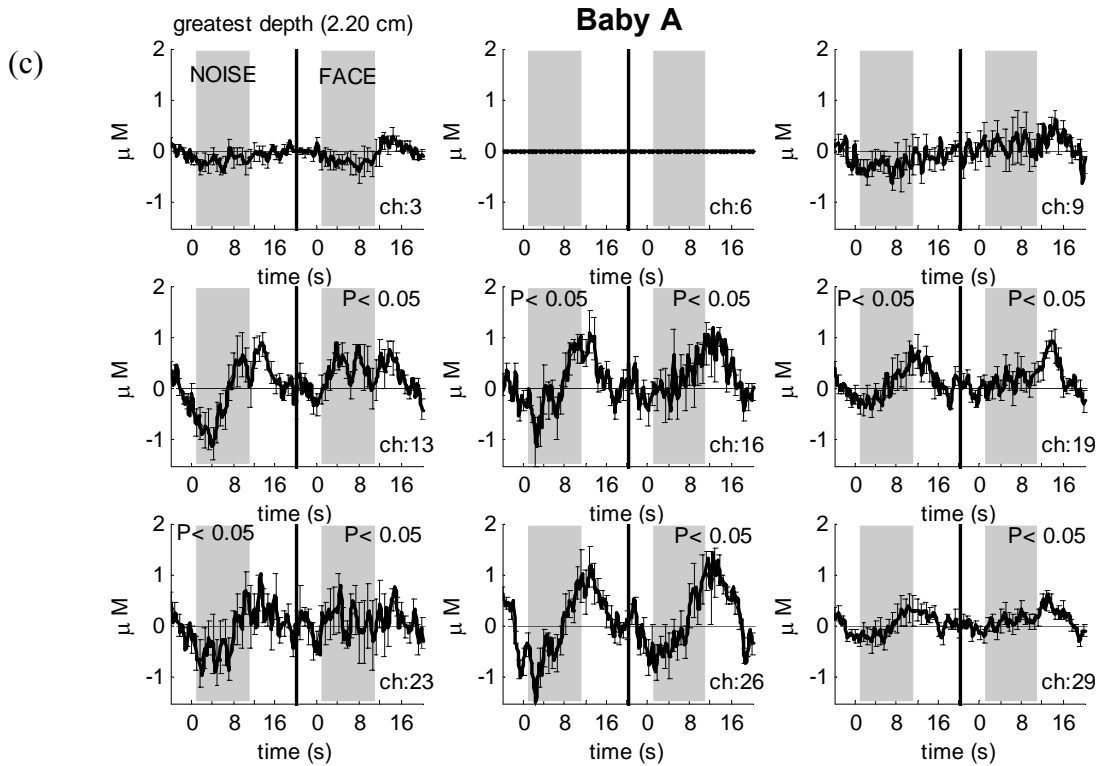


Figure 5: Averaged time course data for changes in HbO_2 for each source detector separation for a single baby (baby A). (a) Shallow depth (1.43 cm s-d separation); (b) intermediate depth (1.78 cm); (c) greatest depth (2.21 cm). Stimulus periods are the shaded areas.

Figure 5 shows the averaged time course of HbO_2 (in mean \pm SE) across 8 face and 9 noise trials for baby A. For this baby, there was activation associated with both face and noise stimulation in the inferior channels of the array at intermediate and greatest depths. Analysis of the maximum HbO_2 increase across the face trials for this baby showed (a) a significant increase in the signal in all the channels in the inferior two rows of the pad (13, 16, 19, 23, 26 and 29) for the greatest depth ($P < 0.05$); and (b) a significant increase in channel 18 in the intermediate source-detector separation. After visual noise onset, there was an increase of HbO_2 in (a) channels 16, 19 and 23 in the greatest depth ($P < 0.05$) and (b) in channels 15 and 25 in the intermediate depth. However, when face activation was compared to noise activation by evaluating the magnitude of the amplitude increase from baseline level in a 4-13 sec post-stimulus onset window (2-tailed T-test),

no significant differences were found. Channel 6 for baby A was discarded from the analysis due to the poor quality of its intensity signals.

We averaged baby A's data across channels by grouping them by source-detector separation to enhance the depth discrimination capabilities of the system by smoothing out the noise (figure 6).

We found that, for baby A, activation with face induced an increase in the HbO₂ signal that was significantly different from baseline only at the greatest depth ($P < 0.05$). Furthermore, this increase was larger with face than with noise stimuli (paired T-test, $P < 0.05$). No significant changes were detected in the depth-averaged HHb signal.

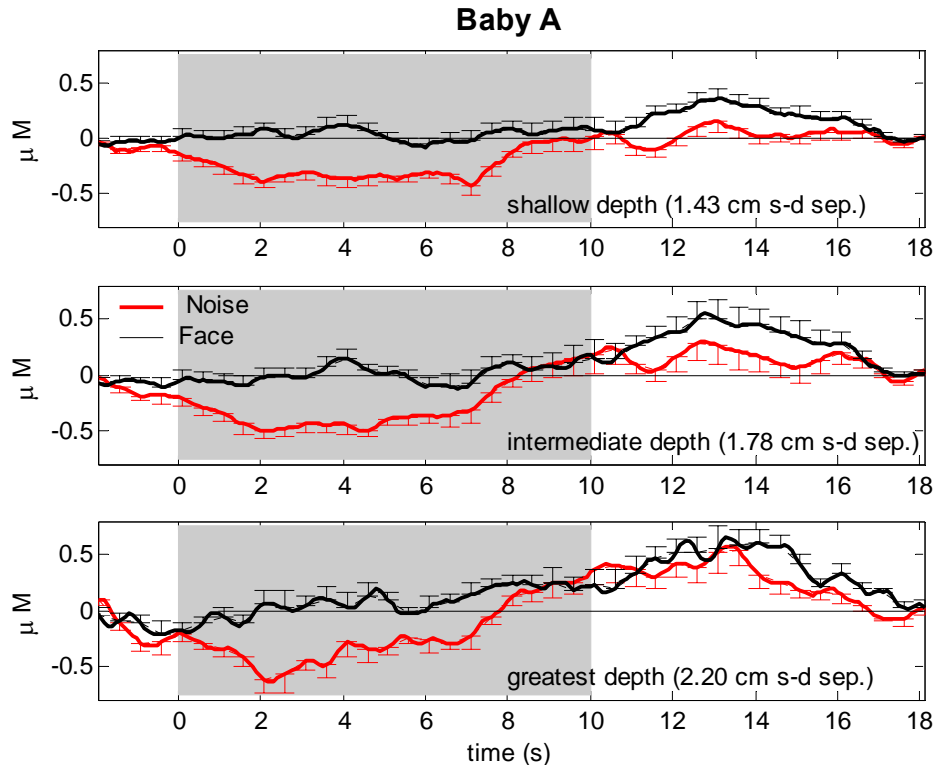


Figure 6: Averaged HbO₂ data for all channels at each source detector separation for a single baby (baby A). Black and red lines represent the HbO₂ time course with face and noise stimulation respectively. The shaded area represents the stimulation period.

Figure 7 shows tomographic reconstructed images of peak HbO₂ changes in baby A in a slice 6

mm thick (averaged between 6 and 12 mm from the surface of the scalp) and with an area of 85 x 85 mm (24 x 24 x 1 in pixels). The top and bottom of the figure correspond to superior and inferior parts of the visual cortex. Figure 7a shows that with face stimulation there is a noticeable increase in HbO₂ in the lower area of the visual cortex spread to both sides of the midline. With visual noise stimulation (figure 7b), the maximum increase in HbO₂ is shifted toward the central region of the visual cortex with a possible region of decrease in HbO₂ adjacent to the maximum HbO₂ increase.

Reconstruction of face HbO₂ change with noise as a reference did not provide any additional information. This was expected as statistical analysis did not find any difference in processing face or noise stimuli in any single channel for baby A.

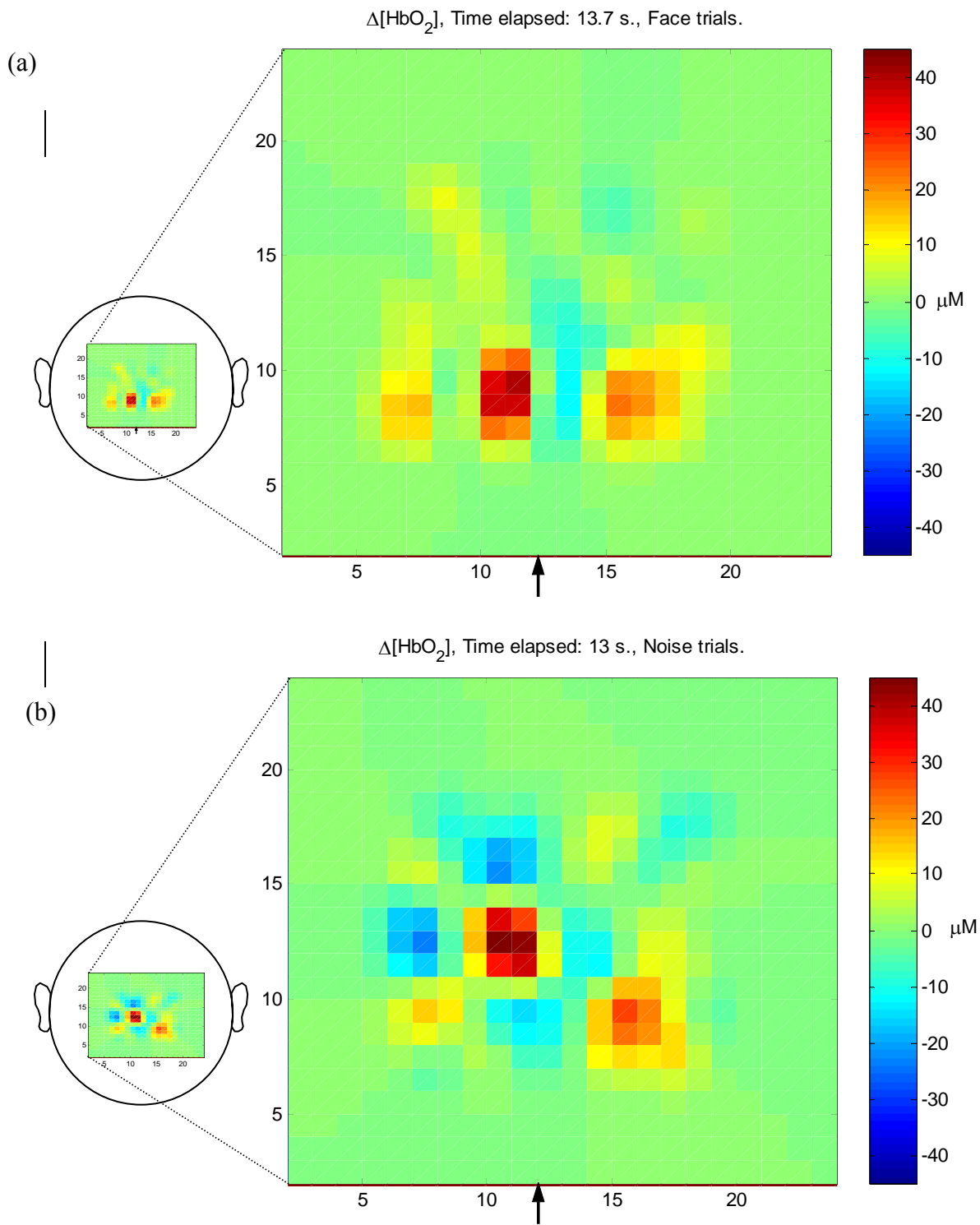


Figure 7: Reconstruction of Baby A's optical topography data (HbO_2 change) from all channels, projected in a single plane ($24 \times 24 \times 1$ pixels). The black arrow on the lower axes represents the approximate position of the midline. (a) Face stimulation. (b) Noise stimulation.

4. Discussion

We used a multi channel NIRS system for measuring haemodynamic response to complex visual stimuli in 4-month-old infants, extending previous work by our group with a dual channel system (Csibra *et al* 2004). The aim of this work was twofold: on the one hand, to differentiate responses to noise and face stimuli in the visual cortex of infants; on the other hand, to test whether our NIRS system was able to pick up haemodynamic activation with some depth resolution.

Additionally, we have tentatively used the multi-distance topography data with a 3D image reconstruction algorithm originally designed for tomography data. The current state of the algorithm is limited in the depth dimension, so our preliminary results show where in the surface of the pad the activation occurs, but only in a slab as thick as the depth sensitivity of the 3 source-detector separations combined.

Our group data suggests that face stimulation activates a larger area of the visual cortex than does visual noise stimulation, as there were more channels with significant HbO₂ increase with face (8 channels) than with noise (1 channel) stimuli. Thus the data shows there are differences between face activation and rest and between noise activation and rest, although these differences are less prominent in the latter case. Of those channels with HbO₂ increase associated with face stimulation, 3 were found at the smallest source-detector separation (shallow depth channels). No significant changes in either HHb or HbT concentration were seen in these channels. At the intermediate depth there was a consistent increase in HbO₂ at one channel (channel 25) with both types of stimulation. At the greatest depth the significant increase in HbO₂ and HbT was spread across the interrogated area, but the haemodynamic response seemed to be stronger at the inferior part of the probe. The spatial localisation of the signal increase observed in the lower half of the pad placed across the midline and centred on Oz (international 10/20 system), and regardless of depth, is in agreement with topography studies where visual stimulation was used with 2-6.5 month old infants (Wilcox *et al* 2005, Taga *et al* 2003). The design of the array (figure 2a) means

that the mid point of the 1.78 cm and 2.20 cm source detector separations occur at the same point making the grid geometry for the intermediate and greatest depths identical. The grid geometry for the shallow depth is different and depends upon more source-detector pairs (12 pairs compared to 9 for the intermediate and greatest depths). Taking this into account, the percentage of channels with significant activation at shallow depth is 8.3%, and intermediate depth is 3.7% and at the greatest depth is 14.8%. It would appear then that the deepest channels seem to be picking up more activation. However it should be pointed out that, although the array is relatively small, the shallow channels do not measure in the exact same positions as the other channels. This may have affected to the differences seen between the number of channels activated at the shallow depth and the other two depths.

Even though the number of channels with face induced increase in HbO₂ was greater than the number of channels with noise induced changes, we were only able to pick up differences between face and noise trials in 3 of those channels, one at each depth. Our results suggest that the difference between the haemodynamic response to face and visual noise stimuli over the visual cortex is expressed more in the change in amplitude of the signal than in its spatial localization. It is possible that these differences could be more easily measured on other parts of the cortex (Kanwisher *et al* 1997).

The observed direction of HbO₂ change agrees with previous NIRS functional activation studies of the visual cortex in infants (Meek *et al* 1998, Wilcox *et al* 2005, Taga *et al* 2003) (in newborns to 3 month-olds). There is some discrepancy in the directional changes in HHb in infant studies, with reports of HHb increasing (Meek *et al* 1998), decreasing (Taga *et al* 2003) or being dependent on location (Wilcox *et al* 2005).

The latency to the peak of HbO₂ increase in our data ranged between 5.1 and 11.6 sec post

stimulus onset. This range is slightly wider than that reported in Taga *et al* (2003), where visual stimulation in infants with a reversing checkerboard induced a response in the visual cortex that peaked between 8 and 10 sec post stimulus onset. A faster rise to peak (4.2 ± 2.0 sec), was reported by Meek *et al* (1998). This difference may be due to the setup used in the latter, with a single source detector pair and a larger separation between them (3.5 cm). The type of stimulus may also influence the speed of the response as olfactory stimulation induced an haemodynamic response starting 5-10 sec after stimulus onset and peaking about 30 sec later (Bartocci *et al* 2000), and object processing in the visual cortex induced a response with a plateau starting 10 sec post stimulus onset that peaked 25-35 sec later (Wilcox *et al* 2005).

A number of groups have been developing NIRS systems that incorporate depth resolution information. Most are time-gated systems (Selb *et al* 2005, Contini *et al* 2006), which have the disadvantage of low sampling rate and long stabilization / cooling times, but the advantage of good spatial resolution and penetration depth (Strangman *et al* 2002). One advantage of our system is that by using software to decode the signal from each source modulated at a different frequency, it is easily adapted to different probe designs, and consequently enables the area and depths of the interrogated volume to be easily tailored to the requirements of any study. For the present study we chose multiple source-detector separations to investigate whether any depth discrimination in the NIRS data could be seen.

When averaging the group data per depth (all channels at each source-detector spacing), we found a significant increase in HbO₂ at intermediate and greatest depths with face stimulation, but no significant increase at any depth with noise stimulation nor a significant difference between face and noise maximum increases. Figure 6 shows the depth averaged results for baby A. In this case, the increase in the signals with face stimulation was significant at the greatest depth and it was larger than with noise stimulation. This suggests there may be some discrimination in the

response as a function of depth. Channel by channel analysis of the changes induced in the signals from baby A also shows predominance of activation at the greatest depths. All channels of the inferior two rows with at the greatest depth show a significant increase in HbO₂ with face activation, whereas only 3 (out of 9) channels at this depth and 3 (out of 9) channels at the intermediate depth show significant increase with noise stimuli (figure 5). These results are in agreement with the group data and represent the typical time course of activation for this type of stimulation. The reason for averaging the signals within each depth was to emphasise the possible differential activation between depths. However, by averaging across channels the amplitude of the signal change is diminished where channels showing activation are averaged with channels where no change is detected. One possible solution would be to translate the channel information onto a 2D map for each depth and then compare activation voxel by voxel. This comparison would work fine between intermediate and greater depths, as the source-detector midpoints are coincident for those 2 depths (see figure 2), but some grid correction would have to be applied at the shallow depth, which has more channels and the theoretical measuring points are differently distributed. Further work is required to determine the best approach to this issue.

Decreases in HbO₂ have been observed in some channels at the beginning of the stimulation period, specially with noise stimuli. These can be seen in the inferior portion of the pad for the intermediate and greatest depths for the single-infant data (figures 5a and 5b). These decreases in HbO₂ may be attributed to the fact that during the rest period the infants were looking at cartoons to keep them focused on the screen. Thus a decrease in HbO₂ may suggest a reduced level of activation at the start of noise stimulation with respect to the cartoons.

In addition to mapping brain activity at each depth, one of the most promising future applications of this topography system is the possibility of reconstructing a 3-dimensional activation image from the data obtained with the different source-detector separations which gather information

from different depths within the cortex. Here we have presented the activation map for a single subject as a 2D slice (24 x 24 x 1 pixels) through a 3D volume at a depth of 6 mm obtained from the multi-distance topography data. More work needs to be done to determine how the topography data, essentially a group of unidimensional measurements, can be transformed into a 3D image. It is important to note that better 2D activation maps could be produced using reconstruction methods that take in account the position and the different spacings between sources and detectors.

The quantitative changes shown in figure 7 (maximum increase of the order of 40 μM) are much larger than the one shown on figure 5 by the HbO_2 time course. This discrepancy can be explained by the problem of partial volumes (Kocsis *et al* 2006, Gibson *et al* 2006), whereby the single channel measurements assume that the change is homogeneous whereas the reconstructed image shows a more accurate spatially localised change. Nevertheless, the magnitude of the HbO_2 increase shown in figure 7 is consistent with the change measured on the motor cortex with optical tomography and reconstructed using the same algorithm with similar parameter settings (Gibson *et al* 2006). However, the exact value of the change should be treated with caution as its absolute value is highly dependent on the reconstruction parameters, in particular on the regularization parameter λ . If instead of 10%, λ was set to 1% then the reconstructed change would not fall within the expected physiological range. The area of activation remains the same regardless of the value of λ .

The simultaneous use of all detectors causes a problem of noise interference between them. There are several ways to address this, and one would be to optimise the source-detector separations (the larger the distance, the worse the signal) and another one would be to sequentially illuminate sources. Further work is required to deal with the volume of data from our system. For example, we need to address the analysis of the multi-channel and multi-subject data, taking into account

all interactions within subjects and between channels that may play a role in the shape of the responses. Another concern that needs to be addressed is the high drop-out rate, which was mainly due to infant discomfort that reduced the amount of time the infant was willing to cooperate. Improving the probe design would not only address this problem but would also help reduce the amount and magnitude of movement artefacts present in the signals. Figure 3 shows the probe used in our studies. The optical fibres of our probe approach the head at a 90° angle. This arrangement has the advantage that the fibres are held away from the subject, preventing the babies from grabbing them, but as the area of contact fibre-pad is small, they are more prone to move with respect to the pad than if the fibres were tangential to the surface. This directly affects the quality of the signals, making this design susceptible to movement artefacts. Work is being done to improve the probe design by terminating each fibre with a 90-degree prism, enabling the fibres to be tangential to the scalp. This should make the probe less susceptible to movement artefacts while still maintaining good contact with the scalp and providing an acceptable level of comfort for the infants. Although movement artefacts were a major contributor to the drop-out rate on our data, other factors such as physiological noise from heart rate, respiration or vasomotion could also interfere with the signals. However, we did not notice this kind of interference in our data. This may be because the lower thickness of the skin compared with the large source-detector separations, together with the smaller vascular compliance in infants (Goodwin *et al* 2004) make these effects less evident.

Conclusion

We have demonstrated that multi channel continuous wave NIRS can be applied to the assessment of functional brain activation in human infants by showing that visual stimulation with faces induces an HbO₂ increase in more channels, thus in a larger area, than visual stimulation with noise. Moreover, we were able to localise where, on the area of the visual cortex probed, the stimuli-related changes occurred. Specifically, we found significant increase of the signal in the inferior region of our probe. The multi-distance NIRS has the potential to provide information about the depth within the cortex where activation originates. Finally, we have shown that it is possible to spatially resolve the location of a specific activation in a 2D plane. We believe the true potential of the method can be achieved when multi-distance measurements are used as input of a 3D reconstruction protocol based on a realistic geometry for the infant head.

Acknowledgement

This research is generously supported by Medical Research Council Programme Grant number G9715587, Medical Research Council Co-operative Group Component Grant number G0400120, European Commission grant (CALACEI) number 12778, and James S. McDonnell Foundation grant number 2100289. We wish to thank all the parents and their children for participating.

References

- Arridge S R 1999 Optical tomography in medical imaging *Inverse Problems* **15** 41-93
- Arridge S R, Hebden J C, Schweiger M, Schmidt F E W, Fry M E, Hillman E M C, Dehghani H and Delpy D T 2000 A method for 3D time-resolved optical tomography *Int. J. Imaging Syst. Technol.* **11** 2-11
- Aslin R N and Mehler J 2005 Near-infrared spectroscopy for functional studies of brain activity in human infants: promise, prospects, and challenges *J. Biomed. Opt.* **10** 011009
- Baird A A, Kagan J, Gaudette T, Walz K A, Hershlag N and Boas D A 2002 Frontal lobe activation during object permanence: data from near-infrared spectroscopy *NeuroImage* **16** 1120-26
- Bartocci M, Winberg J, Ruggiero C, Bergqvist L L, Serra G and Lagercrantz H 2000 Activation of olfactory cortex in newborn infants after odor stimulation: a functional near-infrared spectroscopy study *Pediatr. Res.* **48** 18-23
- Benaron D A, Hintz S R, Villringer A, Boas D A, Kleinschmidt, Frahm J, Hirth C, Obrig H, van Houten J C, Kermit E L, Cheong W-F and Stevenson D K 2000 Noninvasive functional imaging of human brain using light *J. Cereb. Blood Flow Metab.* **20** 469-477
- Bluestone A Y, Abdouleav G, Schmitz C H, Barbour R L and Hielscher A H 2001 Three-dimensional optical tomography of hemodynamics in the human head *Opt. Express* **9** 272-286
- Boas D A, Dale A M and Franceschini M A 2004 Diffuse optical imaging of brain activation: approaches to optimizing image sensitivity, resolution, and accuracy *NeuroImage* **23** S275-88
- Bortfeld H, Wruck E and Boas D A 2007 Assessing infants' cortical response to speech using near-infrared spectroscopy *NeuroImage* **34** 407-15
- Bunce S C, Izzetoglu M, Izzetoglu K, Onaral B, and Pourrezaei K 2006 Functional near-infrared spectroscopy; an emerging neuroimaging modality *IEEE Eng. Med. Biol. Mag.* **6** 54-62
- Colier W N, Quaresima V, Wenzel R, van der Sluijs M C, Oeseburg B, Ferrari M and Villringer A 2001 Simultaneous near-infrared spectroscopy monitoring of left and right occipital areas

- reveals contra-lateral hemodynamic changes upon hemi-field paradigm *Vision Res.* **41** 97-102
- Contini D, Torricelli A, Pifferi A, Spinelli L, Paglia F and Cubeddu R 2006 Multi-channel time-resolved system for functional near infrared spectroscopy *Optics Express* **14** 5418-32
- Csibra G, Henty J, Volein A, Elwell C, Tucker L, Meek J and Johnson M H 2004 Near infrared spectroscopy reveals neural activation during face perception in infants and adults *J. Pediatr. Neurol.* **2** 85-89
- Duncan A, Meek J H, Clemence M, Elwell C E, Tyszczuk L, Cope M and Delpy D T, 1995 Optical pathlength measurements on adult head, calf and forearm and the head of the newborn infant using phase resolved optical spectroscopy *Phys. Med. Biol.* **40** 295-304
- Everdell N L, Gibson A P, Tullis I D C, Vaithianathan T, Hebden J C and Delpy D T 2005 A frequency multiplexed near-infrared topography system for imaging functional activation in the brain *Rev. Sci. Instrum.* **76** 097305
- Farroni T, Johnson M H, Menon E, Zulian L, Faraguna D and Csibra G 2005 Newborns' preference for face-relevant stimuli: Effects of contrast polarity *Proceedings of National Academy of Sciences* **102** 17245-50
- Franceschini M A, Fantini S, Thompson J H, Culver J P and Boas D A 2003 Hemodynamic evoked response of the sensorimotor cortex measured noninvasively with near-infrared optical imaging *Psychophysiology* **40** 548-60
- Fukui Y, Ajichi Y and Okada E 2003 Monte Carlo prediction of near -infrared light propagation in realistic adult and neonatal head models *Applied Optics* **42**, 2881-2887
- Gibson A P, Austin T, Everdell N L, Schweiger M, Arridge S R, Meek J H, Wyatt J S, Delpy D T and Hebden J C 2006 Three-dimensional whole-head optical tomography of passive motor evoked responses in the neonate *NeuroImage* **30** 521-8
- Goffaux V, Jemel B, Jacques C, Rossion B and Schyns P G 2003 ERP evidence for task modulations on face processing at different spatial scales *Cogn. Sci.* **27** 313-25
- Goodwin J A, van Meurs W L, Sa' Couto C D, Beneken J E W and Graves S A 2004 A model for

- educational simulation of infant cardiovascular physiology *Anesth. Analg.* **99** 1655–64
- de Haan M, Pascalis O, and Johnson M H 2002 Specialisation of neural mechanisms underlying face recognition in human infants *Journal of Cognitive Neuroscience* **14**, 199-209
- Halit H, de Haan M and Johnson M H 2003 Cortical specialisation for face processing: face-sensitive event-related potential components in 3- and 12-months-old infants *Neuroimage* **19** 1180-93
- Hintz S R, Benaron D A, Siegel A M, Zourabian A, Stevenson D K and Boas D A 2001 Bedside functional imaging of the premature infant brain during passive motor activation *J. Perinat. Med.* **29** 335-43
- Hoshi Y, Oda I, Wada Y, Ito Y, Yamashita Y, Oda M, Ohta K, Yamada Y and Tamura M 2000 Visuospatial imagery is a fruitful strategy for the digit span backward task: a study with near-infrared optical tomography *Cognitive Brain Research* **9** 339–42
- Hoshi Y 2003 Functional near-infrared optical imaging: Utility and limitations in human brain mapping *Psychophysiology* **40** 511-20
- Jasper H H 1958 Report of the committee on methods of clinical examination in electroencephalography *Electroenceph. Clin. Neurophysiol.* **10** 370-1
- Kanwisher N, McDermott J and Chun M M 1997 The fusiform face area: a module in human extrastriate cortex specialised for face perception *Journal of Neuroscience* **17**, 6336-53
- Kocsis , Herman P and Eke A 2006 The modified Beer–Lambert law revisited *Phys. Med. Biol.* **51** N91-8
- Koizumi H, Yamamoto T, Maki A, Yamashita Y, Sato H, Kawaguchi H and Ichikawa N 2003 Optical topography: practical problems and new applications *Applied Optics* **42** 3054-62
- Kusaka T, Kwada K, Okubo K, Nagano K, Namba M, Ocada H, Imai T, Isobe K and Itoh S 2004 Noninvasive optical imaging in the visual cortex in young infants *Hum. Brain Mapp.* **22** 122–32
- Meek J, Firbank M, Elwell C E, Atkinson J, Braddick O and Wyatt J S 1998 Regional

- hemodynamic responses to visual stimulation in awake infants *Pediatr. Res.* **43** 840-43
- Minagawa-Kawai Y, Mori K, Naoi N and Kojima S 2007 Neural attunement processes in infants during the acquisition of a language-specific phonemic contrast *J. Neurosci.* **27** 315-21
- Nissila I, Kotilahti K, Huutilainen M, Makela R, Lipiainen L, Noponen T, Gavrielides N, Naatanen R, Fellman V and Katila T 2004 Auditory hemodynamic studies of newborn infants using near-infrared spectroscopic imaging *Proc. 26th Annual Intern. Conf. IEEE EMBS San Francisco U.S.A.* 1244-47
- Obrig H and Villringer A 2003 Beyond the visible – Imaging the human brain with light *J. Cereb. Blood Flow Metab.* **23** 1-18
- Okada E, Firbank M, Schweiger M, Arridge S, Cope M and Depty D T 1997 Theoretical and experimental investigation of near-infrared light propagation in a model of the adult head
Applied Optics **36** 21-31
- Pascalis O, de Schonen S, Morton J, Deruelle C and Fabre-Genet M 1995 Mother's face recognition by neonates: A replication and an extension *Infant Behavior and Development* **18** 79-85
- Peña M, Maki A, Kovács D, Dehaene-Lambertz G, Koizumi H, Bouquet F and Mehler J 2003 Sounds and silence: An optical topography study of language recognition at birth *Proc. Natl. Ac. Sci.* **100** 11702-05
- Sakatani K, Chen S, Lichty W, Zuo H and Wang Y 1999 Cerebral blood oxygenation changes induced by auditory stimulation in newborn infants measured by near infrared spectroscopy *Early Hum. Dev.* **55** 229-36
- Schöberl J 1997 NETGEN - An advancing front 2D/3D-mesh generator based on abstract rules *Comput. Visual. Sci.* **1** 41–52
- Selb J, Stott J J, Franceschini M A, Sorensen A G and Boas D A 2005 Improved sensitivity to cerebral hemodynamics during brain activation with a time-gated optical system: analytical model and experimental validation *J. Biomed. Opt.* **10** 011013

- Strangman G, Boas D A and Sutton J P 2002 Non-invasive neuroimaging using near-infrared light *Biol. Psychiatry* **52** 679-693
- Taga G, Asakawa K, Maki A, Konishi Y and Koizumi H 2003 Brain imaging in awake infants by near-infrared optical topography *Proc. Natl. Ac. Sci.* **100** 10722-7
- Takahashi K, Ogata S, Atsumi Y, Yamamoto R, Shiotsuka S, Maki A, Yamashita Y, Yamamoto T, Koizumi H, Hirasawa H and Igawa M 2000 Activation of the visual cortex imaged by 24-channel near-infrared spectroscopy *J Biomed Optics* **5** 93-96
- Tzourio-Mazoyer N, de Schonen S, Crivello F, Reutter B, Aujard Y and Mazoyer B 2002 Neural correlates of woman face processing by 2-month-old infants *Neuroimage* **15** 454-61
- Wilcox T, Bortfeld H, Woods R, Wruck E and Boas D A 2005 Using near-infrared spectroscopy to assess neural activation during object processing in infants *J. Biomed. Opt.* **10** 011010
- Yamashita Y, Maki A and Koizumi H 1999 Measurement system for noninvasive dynamic optical topography *J. Biomed. Opt.* **4** 414-7
- Zhang X, Toronov V Y and Webb A G 2005 Simultaneous integrated diffuse optical tomography and functional magnetic resonance imaging of the human brain *Opt. Express* **13** 5513-5521